M&C 2017 - International Conference on Mathematics & Computational Methods Applied to Nuclear Science & Engineering, Jeju, Korea, April 16-20, 2017, on USB (2017)

FISPACT-II Advanced Nuclear Data Uncertainty Quantification and Propagation Methods

M. Fleming, J-Ch. Sublet and M. R. Gilbert

United Kingdom Atomic Energy Authority, Culham Science Centre, Abingdon OX14 3DB, UK
michael.fleming@ukaea.uk

Abstract - *The inventory code* FISPACT-II *has been designed to quantify nuclear data uncertainties due to incident-particle reactions and propagate these into radionuclide inventory uncertainties so as to quantify uncertainties in observables such as activity, decay heat, source terms and dose rates. These methods have been extended to handle the uncertainties within decay and depletion reactions, in order to handle uncertainty propagation in nuclides that are both created and depleted with non-negligible rates. Coupled with the creation uncertainty propagation, these uncertainties are calculated for BWR MOX conditions with the nuclide Am242m considered as an example and the results are compared with full sensitivity-uncertainty analyses. To handle fission yield uncertainties, which are highly correlated but have no agreed covariance data format, a Total Monte-Carlo method has been developed using a set of sampled GEF-5.3 fission yield files that had been constructed from input parameter variation using distributions determined from a Bayesian method utilising ENDF/B-VII.1 fission yield data. Results are shown for a set of simulations with the Takahama-3 PWR.*

I. INTRODUCTION

Uncertainty quantification and propagation in nuclear simulations is an essential feature that is both increasing in complexity and being more frequently requested by the users of simulation data. Setting aside uncertainties inherent to the simulation methodologies, every physical input to a code has one shared quality: it is a value not precisely representing the real quantity, but based on a set of measurements with a likelihood of being close to the real quantity. The estimation of these likelihoods is translated into an uncertainty quantification and the output of this process can be used to propagate the consequences of this uncertainty into simulations and predicted quantities.

Uncertainties in nuclear data – including nuclear reaction data, thermal scattering, radioactive decay and fission yields – vary tremendously between materials and their applications, but with the advancement of the most sophisticated nuclear physics codes and increase in the power of massively parallel computing, uncertainties can be provided for virtually all parameters. Most impressively, the correlations between different parameters (e.g. different fission yields, cross sections at different energies, emitted particle angles, etc.) are all in principle accessible using modern codes, although the amount of covariance data employed depends entirely on the simulation technique.

II. METHODS

The FISPACT-II inventory and nuclear observables code [1, 2] is a modern simulation system that has been designed to interface directly with any and all nuclear data libraries, including the full TALYS-based Evaluated Nuclear Data Libraries (TENDL) [3] for all incident particles, including neutron, proton, alpha, deuteron and gamma. FISPACT-II possesses a novel combinatorial pathways-based uncertainty propagation method [4] as well as a Monte-Carlo sensitivity-uncertainty functionality to sample based on the full energy-covariance uncertainty data for nuclear reaction data, which has been used to validate the former method [5]. Additional methods have been developed to incorporate and integrate covariance data with Total-Monte-Carlo methods [6], as well as address uncertainty in the depletion of fuel and built-up/burnt nuclides (e.g. plutonium).

While Total-Monte-Carlo (TMC) necessarily requires many parallel simulations and thus increased computational resources, it implicitly offers full uncertainty covariance information. For fission yield uncertainties, this data is an absolute minimum requirement for any meaningful uncertainty propagation and, failing any universally recognised covariance data (and format), TMC represents the best method for propagation of these uncertainties. FISPACT-II can utilise the most yield sets generated using GEF [7], for example the GEFY-5.3 samples [8] or Bayesian-MC yields with ENDF/B-VII.1 [9], JEFF-3.1.1 [10] or other targets. In those papers, FISPACT-II has been use to calculate uncertainties on decay heat benchmarks for which it has been extensively validated [11].

By coupling the TMC sampling of fission yields with the covariance pathways-based uncertainty of FISPACT-II on a full reactor assembly simulation, the full energy-dependent covariances and fission yield covariances may be propagated. In addition, statistical analysis on the pathways-based uncertainties provides the correlation between reaction rate uncertainties and the fission yield uncertainties. These can be calculated on a nuclide or observable (e.g. heat, dose, activity) level, as shown in the next section.

A new functionality for uncertainty quantification in nuclide depletion has been added in the 3-20 code version. While pathways-based uncertainty handles the *production* of radionuclides for the purposes of quantifying uncertainty in radiological quantities, the uncertainty in the depletion of any nuclide – whether through reactions or decays – adds an additional contribution to uncertainty propagation. In comparison with the myriad of possible pathways which produce a nuclide, the depletion occurs only through an easily classed subset of reactions which are precisely the negative diagonal terms of the rate equation matrix.

While FISPACT-II has options to perform full Monte-

Carlo sensitivity analyses, these require prior knowledge of the necessary set of reaction channels that govern the inventory of the nuclide. These may include only a few channels for shorter irradiations, but for many nuclides or irradiation scenarios they may require dozens of reactions combined in a myriad of pathways. To converge full sensitivity calculations with FISPACT-II this may require thousands of calculations for each product nuclide of interest.

A nuclide generally may have some combination of creation and destruction,

$$\frac{dN}{dt} = -\mathsf{D}N + \mathsf{C}, \tag{1}$$

where D is a specific rate while C is a rate of creation, i.e. units of s^{-1} and atoms/s, respectively. While C typically depends on a many quantities including potentially many inventories, decays and reactions, it can be determined by direct reference to the rate equation solutions and the depletion term.

The creation terms in turn have their own associated uncertainties and are the subject of the pathways-based uncertainty analysis in FISPACT-II. To address the depletion uncertainty, FISPACT-II considers three variables with their uncertainties:

λ = total decay rate for the target nuclide
Φ = flux amplitude
σ = total non-scattering cross-section

The depletion specific rate $\mathsf{D} = \lambda + \Phi\sigma$, so using the standard identities for variance of sums or products of random variables and neglecting σ - Φ correlations we obtain:

$$\begin{aligned} var(\mathsf{D}) &= var(\lambda) + \Phi^2 var(\sigma) + \sigma^2 var(\Phi) \\ &\quad + var(\sigma)var(\Phi). \end{aligned} \tag{2}$$

FISPACT-II calculates the fractional uncertainties for half-lives, Δ_λ, and for collapsed cross sections, Δ_σ, which are defined as $\Delta_X = \sqrt{var(X)}/X$. The estimator for the fractional error in the specific rate D is therefore:

$$\Delta_\mathsf{D} = \frac{1}{\mathsf{D}} \sqrt{(\lambda\Delta_\lambda)^2 + (\sigma\Phi)^2(\Delta_\sigma{}^2 + \Delta_\Phi{}^2 + \Delta_\sigma\Delta_\Phi)}. \tag{3}$$

While FISPACT-II is designed to accommodate the uncertainties (including covariances) of incident particle spectra, the current implementation only considers uncertainties in the total flux. Note that a complete covariance treatment of the reaction rate due to cross section energy correlations is implemented, i.e. for a reaction rate R we sum over all energy groups:

$$var(R) = \sum_i \sum_j \phi_i \phi_j cov(\sigma_i, \sigma_j). \tag{4}$$

FISPACT-II outputs the specific depletion rate as well as the percent uncertainty from the equations above. These are also given as a depletion rate using the initial nuclide inventory for each step, as well as a first-order integrated value for the depletion and its uncertainty as a fraction of the final inventory. Note that this is the integrated uncertainty (in atoms) of depletion, which will grow (unbound) monotonically as a percent in pure depletion cases.

In scenarios where a nuclide may be both created and depleted - for example plutonium in a fission reactor, minor actinides, fission products, etc., a combination of both depletion and breeding uncertainties are required. To avoid the complexities and expense of full Monte-Carlo sensitivity-uncertainty analyses, FISPACT-II can be used to calculate depletion and breeding rates with uncertainties. These can be coupled with multiple different approximations. For example, the simplified piece-wise constant equations for a target nuclide of Eq. 1.

If we assume that these terms are constant over the time interval, the solution for this simplified differential equation is simply

$$N_{i+1} = \frac{\mathsf{C}_i}{\mathsf{D}_i} + \left(N_i - \frac{\mathsf{C}_i}{\mathsf{D}_i}\right) \exp\left(-\mathsf{D}_i \Delta t_i\right), \tag{5}$$

and the first order Taylor expansion of the propagated uncertainty yields,

$$\Delta {N_{i+1}}^2 = \left(\frac{\partial N_{i+1}}{\partial \mathsf{D}_i}\right)^2 \Delta {\mathsf{D}_i}^2 + \left(\frac{\partial N_{i+1}}{\partial \mathsf{C}_i}\right)^2 \Delta {\mathsf{C}_i}^2, \tag{6}$$

provides an uncertainty estimate. However, the correlation between creation uncertainty and depletion uncertainty is unambiguous: the depletion rate is proportional to the nuclide inventory, which is directly related to the creation rate. Therefore, the fully-correlated uncertainty is assumed and calculated. These methods have been tested with FISPACT-II to generate coupled uncertainties in simulated actinide inventories for fission fuels, as in Fig. 4, using full depletion-creation correlation and testing against the full sensitivity-uncertainty analysis methods that FISPACT-II offers.

III. RESULTS

To test the uncertainty calculations using the correlated pathways-based production uncertainty and depletion uncertainty, a specific case of physical interest has been selected: Am242m production in a MOX fuel under BWR neutron irradiation conditions. The beginning of life (BOL) spectrum used for these calculations is shown in Fig. 1. To perform the full sensitivity analyses, the relevant reaction pathways must be identified. From the FISPACT-II analyses after a 1000 day irradiation, the set of pathways has been calculated and the major paths identified:

```
path  1   0.886% Np237 ---(R)--- Np238 ---(d)--- Pu238...
                 100.00%(n,g)    100.00%(b-)     100...
path  2   0.938% Pu238 ---(R)--- Pu239 ---(R)--- Pu240...
                 100.00%(n,g)    100.00%(n,g)    100...
path  3  52.162% Pu239 ---(R)--- Pu240 ---(R)--- Pu241...
                 100.00%(n,g)    100.00%(n,g)    100...
path  4  32.193% Pu240 ---(R)--- Pu241 ---(D)--- Am241...
                 100.00%(n,g)    100.00%(b-)     100...
path  5   7.683% Pu241 ---(D)--- Am241 ---(R)--- Am242m
                 100.00%(b-)     100.00%(n,g)
path  6   5.691% Am241 ---(R)--- Am242m
                 100.00%(n,g)
```

These include only those above the 0.5% threshold, although various other complex paths (including loops) contribute less than 0.5% of the total production at any given time

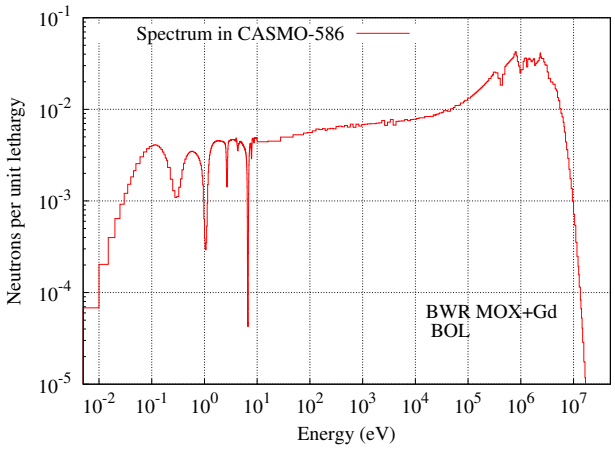

Fig. 1. (Colour online) Neutron spectrum in equal-lethargy units used in the BWR-MOX simulations for Am242m inventory calculations. This is based on CASMO-5 assembly calculations for ATRIUM-10 [12].

in the irradiation scenario considered and therefore those channels are omitted. These are time-dependent, with a % fraction of the produced Am242m inventory presented in Fig. 3. Each of these pathways is identified by the root nuclide and set of reaction channels that sequentially lead to the production Am242m.

The production reaction channels above must be complemented with the depletion channels, which includes fission, neutron capture, inelastic scatter, (n,2n) and (n,3n). In the spectrum used for these calculations, the full energy-correlated uncertainties of Eq. 4 are shown in Table I. For sensitivity-uncertainty calculations, each of these reaction channels must be specified, as well as sampling criteria. For the results shown in Fig. 4, 500 samples from normal distributions per channel are employed, with $\pm 3\sigma$ sampling bounds. The 2σ bands presented in the figure around the uncertainty values represents the distribution of sampled variances - *i.e.* the variance of variance. Note that with this method, not only are potentially many thousands of sampled calculations required, but the convergence of the uncertainties must also be quantified for each analysis.

The results of Fig 4 show several interesting features, where the Am242m inventory notably quadruples over the first 100 days of irradiation and then drops to a pseudo-equilibrium over the next several hundred days. This significant reduction in the production rate of Am242m results in a small, but non-zero apparent decrease in the inventory uncertainty which is verified by the full sampling method. In the true equilibrium case with a creation rate C and specific depletion rate D, the equilibrium inventory is simply the first term of Eq. 5, C/D, and the uncertainty may be calculated simply from this expression. This sets a boundary condition on the nuclide inventory and its uncertainty irrespective of the time-dependent inventory and uncertainties that lead up to that equilibrium state. From the pathways uncertainty for the scenario considered, it is clear that there is no true equilibrium but the 1000 day irradiation results in an inventory near enough to equilibrium

TABLE I. Depletion and production reaction channels for Am242m with cross sections and % uncertainties calculated from the full energy-covariance collapse of Eq. 4 using ENDF/B-VII.1 and the incident neutron spectrum. The Am242m(n,3n) reaction was excluded in sensitivity analyses.

Parent	Daughter	σ (b)	$\Delta\sigma$
Am242m	Fission	231.070	4.418%
Am242m	Am240	1.358E-07	0.000%
Am242m	Am241	2.189E-03	29.925%
Am242m	Am242	7.784	10.785%
Am242m	Am243	43.831	22.495%
Np237	Np238	22.750	4.100%
Pu238	Pu239	10.670	9.500%
Pu239	Pu240	20.886	1.093%
Pu240	Pu241	39.178	0.907%
Am241	Am242m	5.967	4.799%

to see this bounding effect.

In a non-equilibrium state, the uncertainties of the additional components in the inventory solution are added, potentially resulting in an uncertainty greater than the equilibrium case. The expression of Eq. 5 is a simplification that does not present the full inventory solution, but from the cases considered it affords a relatively quick uncertainty propagation method for coupled creation-depletion scenarios that leverages the existing code functionalities.

Most fission processes of interest to reactor physics result in the production of two heavy residuals, often with asymmetric mass. Inventory simulations utilise fission yield data that provides the probability for production of any given residual nuclide following fission. This data is intrinsically correlated with many non-zero matrix elements, as can be seen in Nd148 vector of the the BMC-GEF-5.3 thermal U235 fission yield correlation matrix shown in Fig. 2.

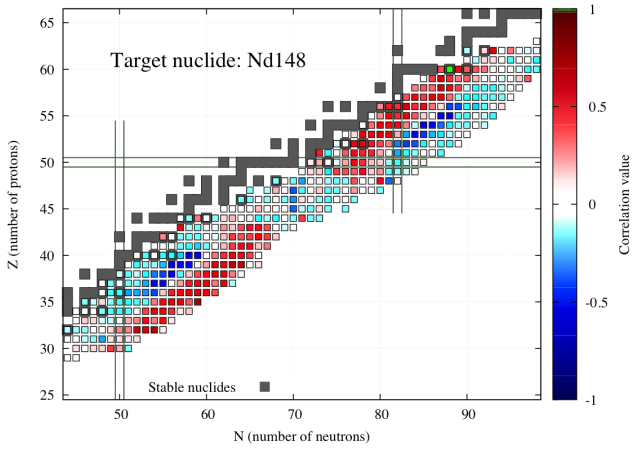

Fig. 2. (Colour online) Nd148 correlation vector from the U235 thermal fission yield correlation matrix, as calculated from the set of BMC fission yields generated using GEF-5.3 and the ENDF/B-VII.1 fission yields as the pseudo-experimental reference file.

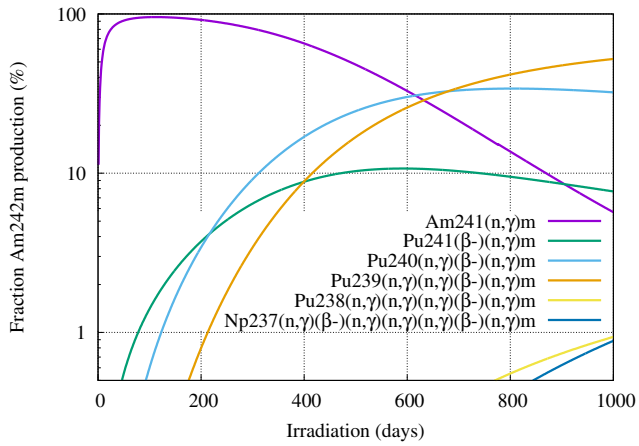

Fig. 3. (Colour online) Fraction contribution from all reaction-decay pathways to Am242m inventory during the 1000 day irradiation at 1.0E+14 n cm^{-2} s^{-1}. These channels are sampled, as well as those depleting the nuclide, within the sensitivity calculations. The time-dependent pathway contributions are utilised by FISPACT-II in the default production uncertainty calculations.

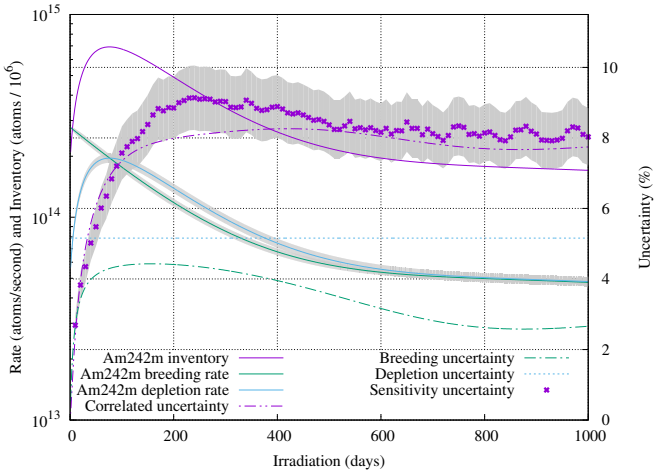

Fig. 4. (Colour online) Coupled breeding-depletion uncertainty analysis of Am242m inventory in a PWR MOX spectrum with constant neutron flux of 1.0E+14 n cm^{-2} s^{-1}. The **DEPLETION** uncertainty is constant for this single incident particle spectrum simulation, while breeding paths and their combined uncertainties are time-dependent. The results from Monte-Carlo sensitivity calculations over all relevant channels are shown for verification, with a 2σ band over the distribution at each time-point for each ensemble of calculations.

In order to couple the reaction and fission yield uncertainties, fission yield uncertainties are required that offer full variance-covariance information. Since these are not available in standard fission yield files, sets of TMC calculations were performed with samples over U235, U238, Pu239 and Pu241 fission yields generated using ENDF/B-VII.1 target BMC fission yields [9].

A set of fission assembly simulations were considered with lattice calculations performed using CASMO-5 [13], including an assembly from the Takahama reactor [14]. The FISPACT-II pathways-based uncertainties using the full ENDF/B-VII.1 covariances were calculated in parallel and statistical analyses over the set of these uncertainties was used to calculate the coupled fission yield with reaction rate uncertainties for all fission products. In this approach each individual calculation uses one of a discrete number of fission yield files. Each of these files has been generated by GEF-5.3 input parameter variation with a set of posterior distributions determined by the Bayesian Monte-Carlo method with ENDF/B-VII.1 fission yield evaluations used as the dataset.

This method provides simulated values and uncertainties for all radionuclides, notably including all of the fission yields and their decay products for all post-irradiation cooling times ranging from seconds to decades and beyond. These are shown in the 1 second cooling of all fission products in Fig. 5 and the coupled uncertainties for each of these are calculated for all nuclides, as shown in Fig. 6.

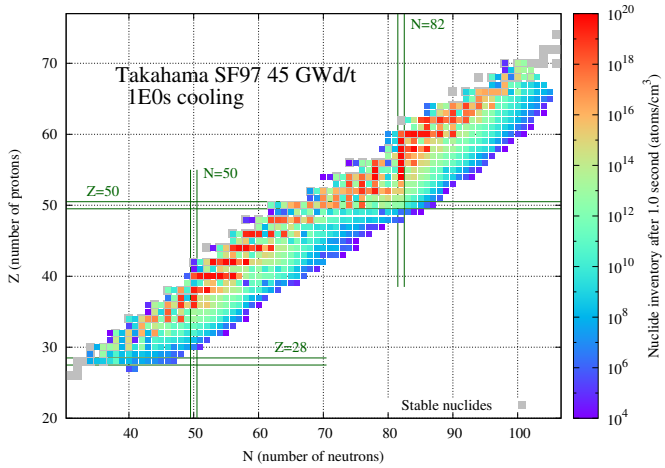

Fig. 5. (Colour online) Takahama-3 SF97 after 45 MWd/THM using ENDF/B-VII.1 nuclear data for reaction covariances and BMC sampled fission yields, showing the full nuclide inventory after 1 second cooling. Note that FISPACT-II tracks all fission products and their decay processes.

FISPACT-II has been designed to quantify uncertainties in the essential responses, such as dose rates and decay heats, and by default identifies the dominant nuclides at all time-steps. The pathways-based production uncertainty is calculated using the incident-particle covariance data as in the previous section. Coupling the TMC fission yield sampling provides both the missing fission yield uncertainty and allows the calculation of the coupled uncertainty due to fission product yields from

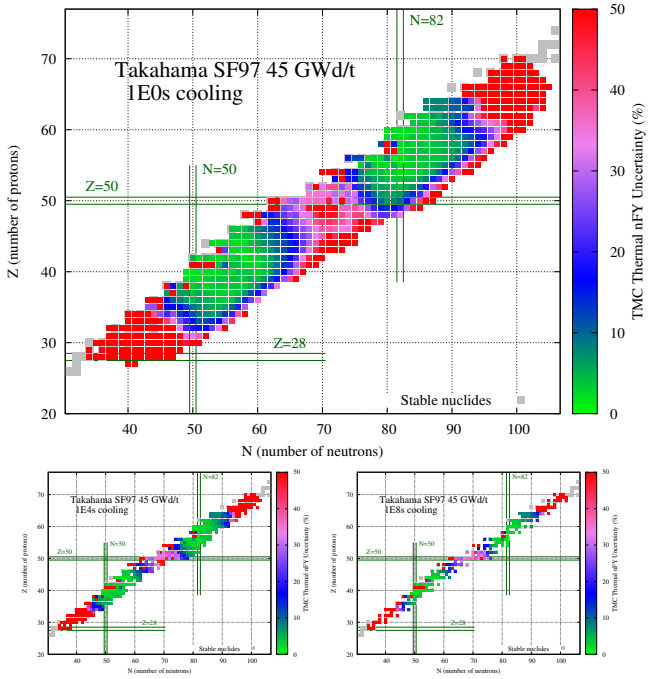

Fig. 6. (Colour online) Takahama-3 SF97 after 45 MWd/THM using ENDF/B-VII.1 nuclear data for reaction covariances and BMC sampled fission yields, showing the propagated uncertainty for each of the fission yields simulated by FISPACT-II at cooling times of 1 second, 10^4 seconds (2.8 hours) and 10^8 seconds (3.2 years).

multiple fissioning nuclides. When two or more fuel nuclides produce the same product, uncertainties calculated through the FISPACT-II production uncertainty method will vary with the fission yield file sampling, producing this coupled effect as shown in Fig. 7 for a selection of cooling times.

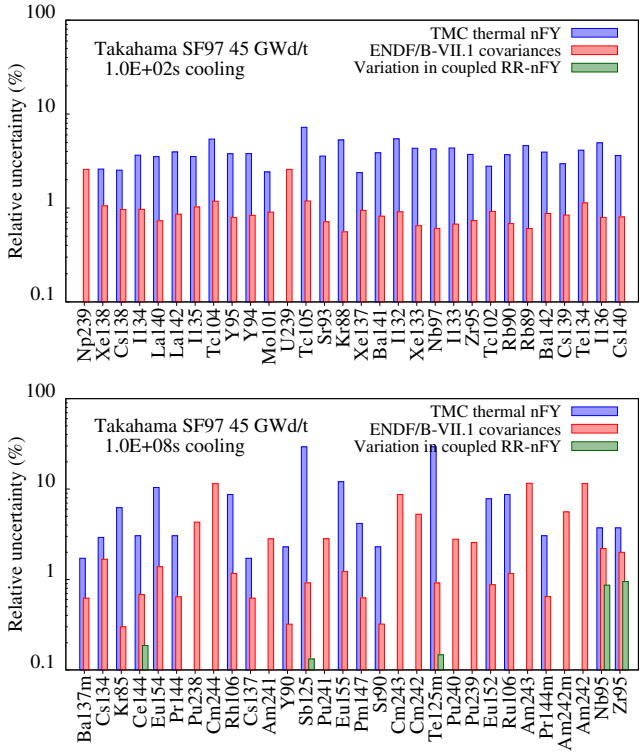

Fig. 7. (Colour online) Takahama-3 SF97 after 45 MWd/THM using ENDF/B-VII.1 nuclear data for reaction covariances and BMC sampled fission yields, showing the dominant nuclides at 100 and 10^8 s cooling with their fission yield and reaction rate uncertainties, as well as the coupled variation from variation of both reaction channels and fission yields.

In addition to the nuclide-by-nuclide uncertainties, integral quantities such as decay heat may be calculated and uncertainties propagated, as shown in Fig 8. Note that while the uncertainties for many radionuclides are relatively large (e.g. >50%), the variation in the fission yields itself varies quite strongly with the yield, so that those with fission yields greater than 1.0E-03 typically have very small uncertainties.

IV. CONCLUSIONS

The FISPACT-II system brings many new capabilities to the long established family of inventory codes. At the core of the main code is a rate equation solver that exploits the most advanced physics provided in modern nuclear data forms, including the full variance-covariance data. Coupled creation-destruction uncertainty quantification and propagation methods have been implemented and tested against full sensitivity-uncertainty methods that are already built into FISPACT-II but

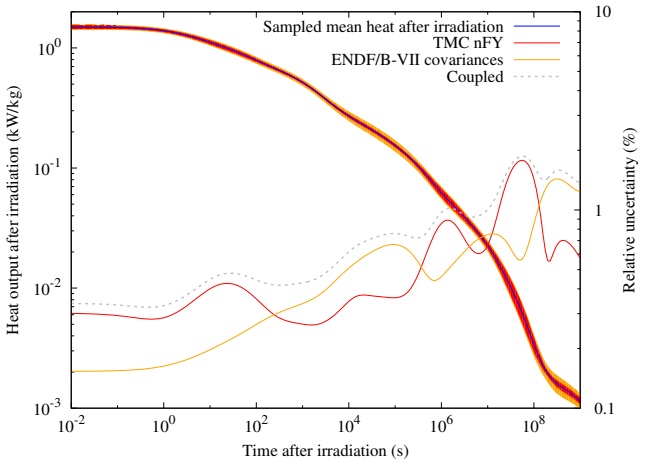

Fig. 8. (Colour online) Takahama-3 SF97 after 45 MWd/THM using ENDF/B-VII.1 nuclear data for reaction covariances and BMC sampled fission yields for ^{235}U, ^{238}U, ^{239}Pu and ^{241}Pu.

require considerable computational expense. The ability to read and simulate using any of the sampled BMC fission yield files offers uncertainty propagation that implicitly includes all fission yield correlations. Coupling these two provides robust quantification of uncertainties for all radionuclides, subject to the quality of the reaction and fission yield covariance data provided in the nuclear data files.

V. ACKNOWLEDGMENTS

This work was funded by the RCUK Energy Programme under grant EP/1501045. We are grateful to D. Rochman and O. Leray for providing neutron spectra for a variety of systems and for both creating and distributing the BMC fission yield files.

REFERENCES

1. J.-CH. SUBLET, J. EASTWOOD, J. MORGAN, M. FLEMING, and M. GILBERT, "FISPACT-II User Manual," Tech. Rep. UKAEA-R(11)11 Issue 8, UKAEA (Dec. 2016), http://fispact.ukaea.uk.
2. J.-CH. SUBLET, J. EASTWOOD, J. MORGAN, M. GILBERT, M. FLEMING, and W. ARTER, "FISPACT-II: An Advanced Simulation System for Activation, Transmutation and Material Modelling," *Nuclear Data Sheets*, **139**, 77 – 137 (2017), special Issue on Nuclear Reaction Data.
3. A. KONING and D. ROCHMAN, "Modern Nuclear Data Evaluation with the TALYS Code System," *Nuclear Data Sheets*, **113**, *12*, 2841 – 2934 (2012), special Issue on Nuclear Reaction Data.
4. J. EASTWOOD, J. MORGAN, and J.-CH. SUBLET, "Inventory Uncertainty Quantification using TENDL Covariance Data in Fispact-II," *Nuclear Data Sheets*, **123**, 84 – 91 (2015).
5. ARTER, W. AND MORGAN, J.G., "Sensitivity Analysis for Activation Problems," in "Joint International Conference on Supercomputing in Nuclear Applications and Monte Carlo 2013," (2014), p. 02404, http://dx.doi.org/10.1051/snamc/201402404.
6. A. KONING and D. ROCHMAN, "Towards sustainable nuclear energy: Putting nuclear physics to work," *Annals of Nuclear Energy*, **35**, *11*, 2024 – 2030 (2008).
7. K.-H. SCHMIDT, B. JURADO, C. AMOUROUX, and C. SCHMITT, "Special Issue on Nuclear Reaction Data General Description of Fission Observables: GEF Model Code," *Nuclear Data Sheets*, **131**, 107 – 221 (2016).
8. K.-H. SCHMIDT, "GEFY: GEF-based fission-fragment Yield library in ENDF format," (2016), www.khs-erzhausen.de/GEFY.html.
9. D. ROCHMAN, O. LERAY, A. VASILIEV, H. FERROUKHI, A. KONING, M. FLEMING, and J. SUBLET, "A Bayesian Monte Carlo method for fission yield covariance information," *Annals of Nuclear Energy*, **95**, 125 – 134 (2016), https://tendl.web.psi.ch/tendl_2015/randomYields.html.
10. O. LERAY, D. ROCHMAN, M. FLEMING, J.-CH. SUBLET, A. KONING, A. VASILIEV, and H. FERROUKHI, "Fission yield covariances for JEFF: a Bayesian Monte Carlo method," in "ND 2016 International Conference on Nuclear Data for Science and Technology," (2016).
11. M. FLEMING and J.-CH. SUBLET, "Validation of FISPACT-II Decay Heat and Inventory Predictions for Fission Events," Tech. Rep. CCFE-R(15)28, CCFE (2015).
12. O. LERAY, P. GRIMM, H. FERROUKHI, and A. PAUTZ, "Quantification of code, library and cross section uncertainty effects on the void reactivity coefficient of a BWR UO2 assembly," in "PHYSOR-2014, Kyoto, Japan, September 28 - October 3," (2014).
13. D. ROCHMAN, O. LERAY, M. HURSIN, H. FERROUKHI, A. VASILIEV, A. AURES, F. BOSTELMANN, W. ZWERMANN, O. CABELLOS, C. DIEZ, J. DYRDA, N. GARCIA-HERRANZ, E. CASTRO, S. VAN DER MARCK, H. SJÃŰSTRAND, A. HERNANDEZ, M. FLEMING, J.-C. SUBLET, and L. FIORITO, "Nuclear Data Uncertainties for Typical {LWR} Fuel Assemblies and a Simple Reactor Core," *Nuclear Data Sheets*, **139**, 1 – 76 (2017), special Issue on Nuclear Reaction Data.
14. C. SANDERS and L. GAULD, "Isotopic analysis of high-burnup PWR spent fuel samples from the Takahama-3 reactor," Tech. Rep. NUREG/CR-6798, ORNL/TM-2001/259, Oak Ridge National Laboratory (2003).